UNIVERSITY OF CALIFORNIA, SAN DIEGO

The Role of PRMT5/MEP50 in p100-centric κBsome Assembly

A Thesis submitted in partial satisfaction of the requirements
for the degree Master of Science

in

Chemistry

by

Boqing Gu

Committee in charge:

Professor Gourisankar Ghosh, Chair
Professor Rommie Amaro
Professor Elizabeth Komives
Professor Ulrich Muller

2017

The Thesis of Boqing Gu is approved, and it is acceptable in quality and form for publication on microfilm and electronically:

_____

_____

_____

_____

Chair

University of California, San Diego

2017

DEDICATION

This Thesis is dedicated to Wenjia Huang, my beloving girlfriend for her unwavering support, patience and encouragement throughout my graduate study. Thank you very much.

TABLE OF CONTENTS

LIST OF ABBREVIATIONS

ARD	ankyrin repeats domain
BME	β-mercaptoethanol
cDNA	complementary DNA
DD	dimerization domain
DeD	death domain
DTT	dithiothreitol
ECL	enhanced chemiluminescence
GRR	glycine rich repeat
IκB	inhibitor of NF-κB
IKK	inhibitor of NF-κB kinase
IPTG	isopropyl β-D-1-thiogalactopyranoside
kDa	kilodalton
MEP50	methylosome protein 50
MOI	multiplicity of infection
MW	molecular weight
NEMO	NF-κB essential modulator
NF-κB	nuclear factor kappa B

NIK	NF-κB inducing kinase
NLS	nuclear localization sequence
NTA	nitrilotriacetic acid
NTD	N-terminal domain
PAGE	polyacrylamide gel electrophoresis
PEST	sequence rich in Pro, Glu, Ser and Thr
PIC	protease inhibitor cocktail
PMSF	phenylmethylsulfonyl fluoride
PRMT5	protein arginine methyltransferase 5
RHR	Rel homology region
SAM	S-Adenosyl methionine
Sf9	*Spodoptera frugiperda* 9
SDS	sodium dodecyl sulfate
TAD	transcriptional activation domain

LIST OF FIGURES

LIST OF TABLES

ACKNOWLEDGEMENT

I would like to thank my advisor, Dr. Gourisankar Ghosh, who has continually supported, motivated, and encouraged me to do my best through my study in his lab. Without his help, I could not have made it such far. I am very grateful for his patience, challenges, humor, and even sometimes harshness. He has been a great mentor who has left a great impact and legacy in my life.

I would like to thank my thesis committee advisor, Dr. Elizabeth Komives who has been a wonderful teacher and a friend. She was my professor for biochemistry class and later biophysical chemistry class. During several critical life moments, her advices light up my path to be a scientist. Through her passion for teaching and love for biochemistry, I devote myself into this field, too.

I would like to thank my other thesis committee advisor, Dr. Ulrich Muller who brings various seminar speakers from all fields of biochemistry in the first year graduate class. It is these talks that inspire me to continue work on my study.

I would also like to thank the following past and present members of the Ghosh Lab for their tremendous guidance and assistance: Dr. Yidan Li, Dr. Anup Mazumder, Dr. Vivien Wang, Dr. Mari Mulero-Roig, Dr. Tapan Biswas, Dr. De-Bin Huang, Dr. Huong Thien Nguyen, Qian Du, Mike Fernandez, Samantha Cohen, Kyle Shumate, Yunshu Song, Sonjiala Hotchkiss, Daniel Kim, Shandy Shahabi, and Sarah Fulop.

Finally, I would like to thank my family and friends who have supported me immensely.

The result section in part is currently being prepared for submission for a future publication of the material. The thesis author was the primary researcher and one of co-authors of this material.

ABSTRACT OF THE THESIS

The Role of PRMT5/MEP50 in p100-centric κBsome Assembly

by

Boqing Gu

Masters of Science in Chemistry

University of California, San Diego, 2017

Professor Gourisankar Ghosh, Chair

It is well known that nearly half of all NF-κB subunits are inhibited by the precursor inhibitors, p100 and p105, whereas the other half are by classical IκBs (IκBα, IκBβ and IκBε). Our laboratory showed, through experiments done *in vivo*, that inhibition by these precursors requires their association with multiple NF-κB molecules including their processed products resulting in the formation large complexes of MW about 600 kDa to 800 kDa. These large complexes are known as kappaBsomes (κBsomes). p100-centric κBsomes are intriguing in that they must bind to RelB, a member of the NF-κB family. In

contrast, p105-centric κBsomes do not interact with RelB. However, effort to form p100-centric κBsome by co-expressing p100, RelB and RelA were not successful. Although they associated and formed a complex, neither the size nor the stability matched *in vivo* results. This led to the identification of PRMT5 as a possible partner of p100-κBsome. To further study this association,I co-expressed p100, RelB, RelA, PRMT5 and MEP50 (partner of PRMT5) in the baculovirus expression system and tested the stability of their association through multiple chromatographic purification steps. I observed that the p100-κBsome and PRMT5:MEP50 complexes associate with each other, but this association is strong. We observed that the complex tends to disassemble as the purification progresses. This resulted in very little complex yield after the final step of purification. I conclude that the association between the two complexes is dynamic involving weak, transient interactions. To test the functional relevance of this possible association, I tested phosphorylation of p100 by NIK:IKK1 in the presence or absence of its NF-κB and PRMT5 partners. I found that the PRMT5:MEP50 complex partly inhibits p100 phosphorylation and this inhibition is enhanced in the presence of RelB. p100 is not phosphorylated in the five-protein complex (p100, RelA, RelB, PRMT5 and MEP50). These results suggest that the dynamic association of PRMT5:MEP50 complex is necessary to prevent aberrant phosphorylation of p100 in unstimulated cells.

I. Introduction

A. NF-κB Transcription Factors

Nuclear Factor Kappa B (NF-κB) was discovered in David Baltimore's laboratory in 1986 as a dimeric transcription factor composed of two polypeptides with molecular weight approximately 50 kDa (p50) and 65 kDa (p65). They showed that the dimer resides in the cytoplasm bound to an inhibitor protein, known as IκB (inhibitor of NF-κB) (Sen and Baltimore, 1986). Extracellular stimuli induce degradation of IκB resulting in the release of NF-κB. Subsequent studies identified a protein kinase that is activated upon stimuli and is responsible for phosphorylation of IκB and its subsequent degradation (Figure 1.1) (Pahl, 1999).

NF-κB was originally thought to be present solely in immune cells and functioned in the immune response against environmental challenges. It is now known to be a family of proteins that is present in almost all cell types and is responsible for transcription of a large number of genes, including genes involved in growth, development, apoptosis, stress responses, and innate and adaptive immunity (Baeuerle and Baltimore, 1996; Baeuerle and Henkel, 1994; Baldwin, 1996; Ghosh et al., 1998). NF-κB factors regulate both the activation and repression of genes by binding to short homologous DNA sequences known as κB sites (Chen et al. 1998). These NF-κB target genes in turn carryout diverse biological functions such as cellular immunity and inflammation, cell survival and apoptosis, and proliferation. NF-κB mostly remains inactive in resting cells (Oeckinghaus and Ghosh, 2009). Diverse stimuli activate NF-κB by engaging with cell surface receptors and orchestrating a series of reactions as discussed below.

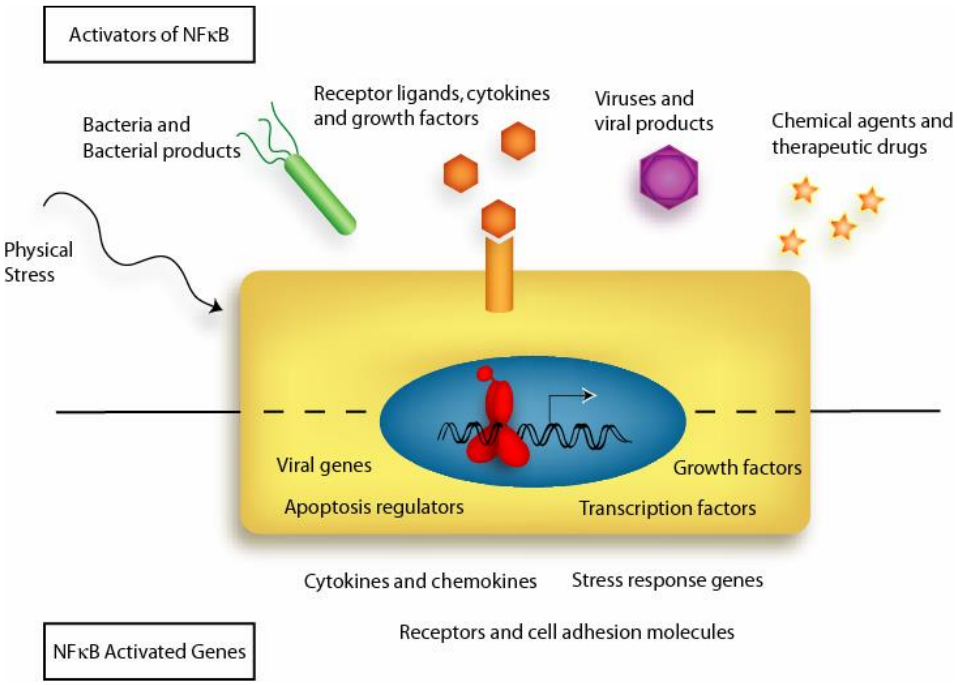

Figure 1.1 Activators and responses of NF-κB mediated transcription.
Schematic representation of a cell. The major NF-κB activators are shown in the top half of the figure, and the activated gene are shown in the lower half (separated by dash line and model of NF-κB dimer binding to DNA).

B. NF-κB Family and DNA Binding

The NF-κB family is composed of five polypeptides, p50, p52, p65 (RelA), cRel and RelB (Figure 1.2). These proteins share a homologous N-terminal segment of approximately 300 residues. This homologous region is referred to as the Rel Homology Region (RHR) (Baeuerle and Baltimore, 1996; Baldwin, 1996). The RHR is responsible for subunit dimerization, DNA binding and nuclear entry. Of these subunits, p50 and p52 do not contain a transcriptional activation domain (TAD). Therefore, p50 and p52 homodimers primarily act as transcriptional repressors. p50 and p52 are generated from their precursors, p105 and p100, respectively (Bours et al., 1990; Ghosh and Baltimore, 1990; Kieran et al., 1990). Dimers containing RelA, cRel and RelB are able to activate transcription, however, they also act as transcription repressors (Hoffmann et al., 2006). Although there can be fifteen possible combinatorial dimers from five monomers, not all dimers have been observed in the cell (Hayden and Ghosh, 2004). Therefore, propensity towards dimerization provides one level of regulation. For instance, the most abundant dimer is the p50:RelA heterodimer which is arguably the most stable (Chen et al. 1998). RelB:RelB homodimer, RelA:RelB and cRel:RelB heterodimers do not exist *in vivo* suggesting these dimers are highly unstable (Ruben et al. 1992; Ryseck et al. 1995).

The RHR folds into two distinct domains, the N-terminal domain (NTD) is responsible for sequence-specific DNA binding and the C-terminal domain is responsible for subunit dimerization. The dimerization domain (DD) is also responsible for sequence non-specific DNA binding. The C-terminus of RHR contains a 15-residue long flexible segment. The last four basic residues comprise the nuclear localization signal (NLS).

NF-κB dimers specifically bind to 9 to 11 base pair DNA sequences with strong

similarity. Consensus of these sequences is 5'-(G)GGRNNNYCC(C)-3'. The central base pairs (underlined) is located at the pseudodyad axis that divides the sequences into two half-sites. Each subunit of a dimer binds to one half site. The G/C core sequences at the flanking region is the most characteristic feature of κB sites whereas the central sequences can be variable (Ghosh et al., 1995). p50 and p52 homodimers prefers G/C in the central region but RelA and cRel homodimers prefer A/T at the central region (Chen et al. 1998; Chen et al. 2000).

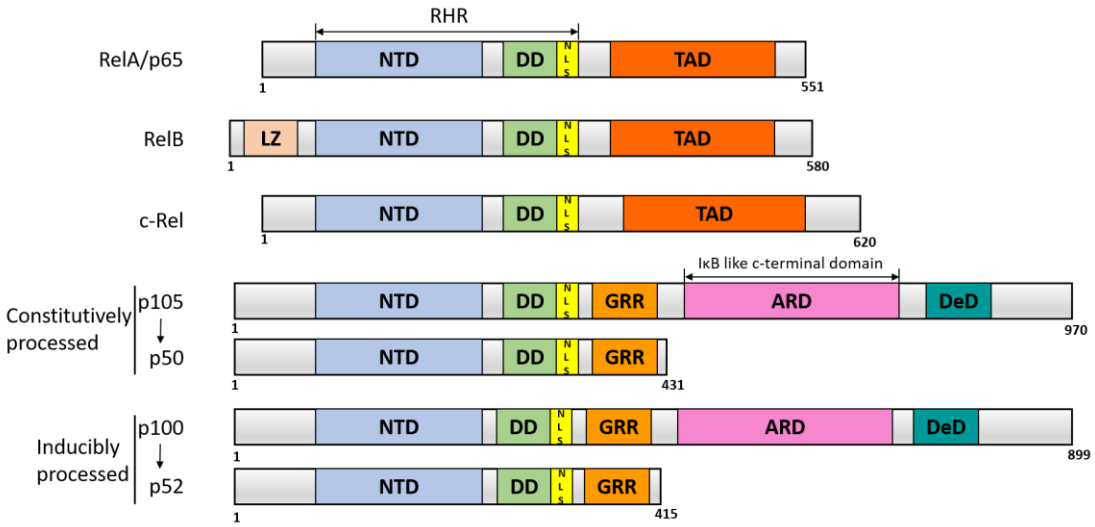

Figure 1.2. A schematic representation of members of the NF-κB family.
The RHR of NF-κB are shown in blue (N-terminal domain) and green (dimerization domain), the transactivation domains in red-orange, the GRR in orange, and leucine zipper in pale brown. The location of the NLS is also labeled. For p105 and p100 the ARDs are shown in pink and death domains in dark green.

C. The IκB Family

IκB proteins share a homologous ankyrin repeat domain (ARD). The ARD is composed of six-seven 33-residue long peptide sequences. Although the ARD is present in hundreds of proteins, each family of ARD proteins deviates differently from the consensus of ankyrin repeat (AR) sequence. Eight family members comprise the IκB family- IκBα, IκBβ, IκBε, p100/IκBδ, p105/IκBγ, Bcl3, IκBζ/MAIL, and IκBNS. These proteins can be further separated into three sub-families based on their structural and functional features (Oeckinghaus and Ghosh, 2009). IκBα, IκBβ and IκBε belong to the classical sub-family, p100/IκBδ and p105/IκBγ comprise the precursor sub-family; and Bcl3, IκBζ and IκBNS comprise the atypical sub-family (Figure 1.3).

Classical and precursor inhibitors are responsible for the inhibition of all TAD containing NF-κB subunits. Whereas all inhibitors inhibit RelA and cRel, RelB is inhibited exclusively by p100/IκBδ. The atypical inhibitors bind to p50 and p52 homodimers. It was originally thought that they are not inhibitors, but instead function as coactivators of p50 and p52 homodimers which lack TAD. It has recently been revealed that these proteins also inhibit transcription by forming ternary complexes with a sub-class of DNA sequences (Schuster et al., 2013). More work is required to understand the detailed mechanism of actions of the atypical inhibitors.

The most well studied of the IκB inhibitors is IκBα. IκBα has the strongest affinity towards the p50: RelA heterodimers and it also efficiently inhibits RelA homodimer and cRel homodimers and heterodimers. Various biophysical methods including x-ray crystallography and H/D exchange coupled to mass spectrometry have interrogated how IκBα inhibits NF-κB dimers (Huxford et al., 1998; Malek et al., 2003). One molecule of

IκBα interacts with one NF-κB dimer forming a 1:1 complex with an affinity of nearly ~10 pM (K_D). In the complex, the NLS of RelA is bound strongly to the first three AR of IκBα. The C-terminal PEST (sequence rich in Pro, Glu, Ser and Thr) sequence interacts strongly to the bottom of the DD and NTD of RelA. The ARD primarily interacts with the dimeric surface formed by the two monomers(Huxford et al., 1998). These studies explain how IκBα prevents p50:RelA heterodimer from going to the nucleus and binding DNA. Apparently, IκBβ and IκBε adopt similar mechanisms to inhibit NF-κB. It is however clear that IκBβ has a higher propensity to inhibit RelA homodimer.

All IκB proteins barring IκBβ are targeted by NF-κB for post induction synthesis. Therefore, IκB proteins inhibit NF-κB at two levels: initially at the resting state of cells and then post induction. For instance, IκBα is synthesized within one hour of induction and the newly synthesized IκBα enters the nucleus and actively removes NF-κB from any promoters. This 'negative feedback' regulation is extremely important for preventing NF-κB from regulating gene expression for an unlimited amount of time. Constitutive activation of NF-κB leads to constitutive expression of cell survival and proliferation genes, ultimately resulting in several diseases such as cancers (Oeckinghaus and Ghosh, 2009).

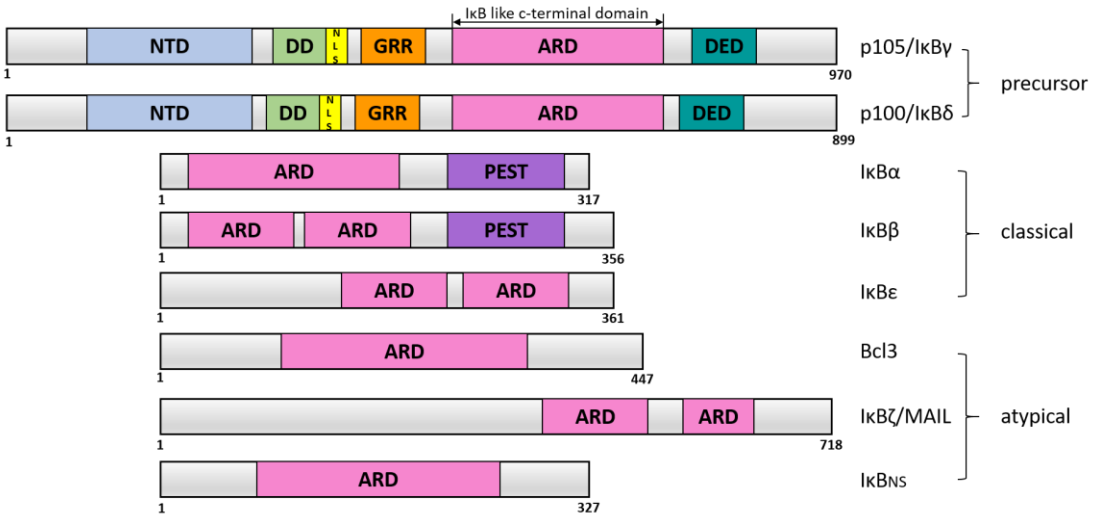

Figure 1.3. A schematic representation of members of the IκB family.
For precursor IκBs the ankyrin repeat domains (ARDs) are shown in pink and death domains in dark green. For IκBα and IκBβ the PEST region are shown in purple.

D. NF-κB Activation Pathways

There are two major signaling pathways leading to activation of NF-κB factors: canonical and non-canonical (Figure 1.4). A set of stimuli activates RelA and cRel dimers through degradation of classical IκBs and p105/IκBγ (Oeckinghaus et al., 2011**)**. These stimuli activate the IκB Kinase 2/b (IKK2/b) subunit of the IKK complex. The non-canonical pathway activates the IKK1 subunit of the IKK complex. In addition to the catalytic IKK1 and 2 subunits, IKK complex also contains an adapter protein known as NEMO (NF-κB Essential Modulator) (Karin and Ben-Neriah, 2000). Whereas the activation of IKK2 through canonical pathway requires NEMO, activation of IKK1 through non-canonical pathway does not require NEMO. Instead, the kinase NIK (NF-κB Inducing Kinase) is required to activate IKK1 (Karin and Ben-Neriah, 2000). The precise mechanism of how the canonical and non-canonical pathways activate IKK2 and IKK1, respectively, is not clear. The only fact that is clear is that the canonical pathway induces the synthesis of Lys63-linked or linear poly-ubiquitin chains which interact with NEMO. This interaction is critical for IKK2 activation through phosphorylation of two activation loop serines (Ser177 and Ser181) (Delhase et al., 1999).

In resting cells, NIK is continuously degraded by the actions of several Lys48 ubiquitin ligases and proteasome (Vallabhapurapu and Karin, 2009). Non-canonical signaling decouples the NIK-E3 ligase interaction, hence stabilizes NIK. NIK then interacts with IKK1 and activates it through phosphorylation of its activation loop serines (Ser176 and Ser180). The main goal of non-canonical pathway is the induction of p100 processing into p52. The resulting NF-κB dimers through non-canonical signaling are the p52 homodimer and p52:RelB heterodimer. The NIK:IKK1 complex phosphorylates three

serines (Ser866, Ser870 and Ser872) of p100 (Xiao et al., 2001). These phosphorylation events are critical for p100 processing mechanism. In many cancers, NIK is constitutively active, thereby maintaining high levels of p52. Enhanced level of p52 homodimers and p52:RelB heterodimers, which regulates many genes involved in the cell cycle. Constitutive activation of these genes is key to a large number of malignancies (Xiao et al., 2001).

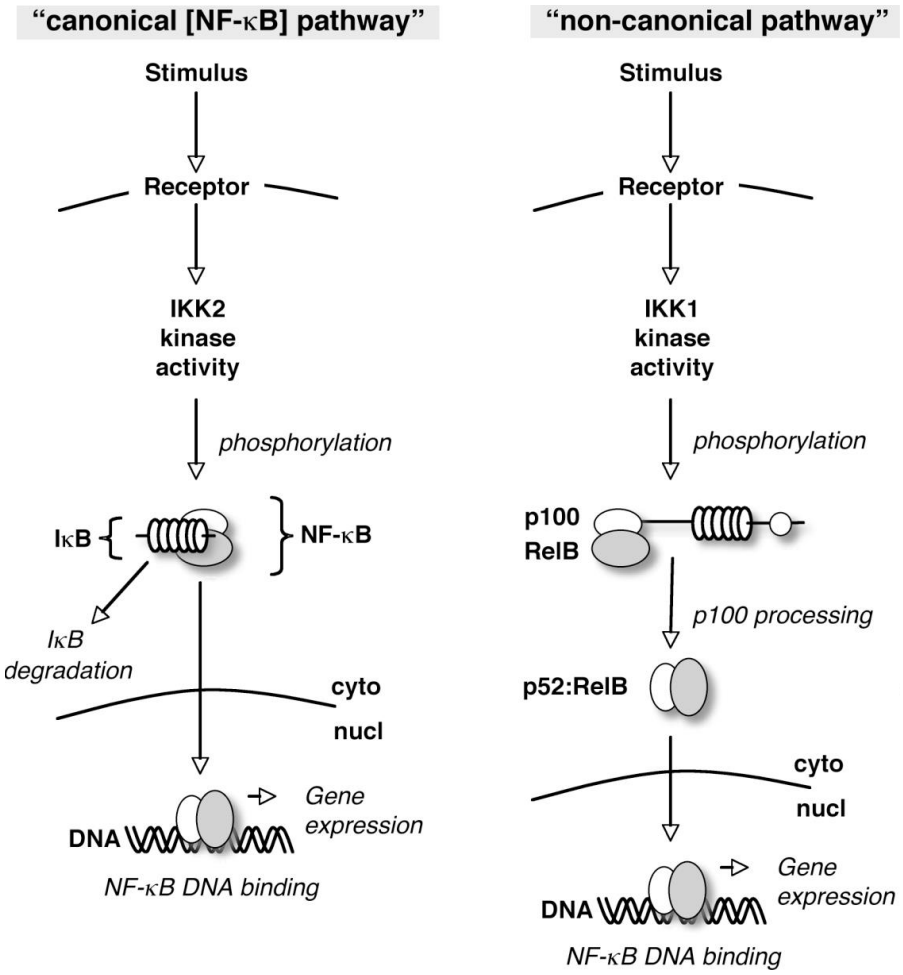

Figure 1.4. Two major NF-κB activation pathways.
IκB proteins regulate NF-κB activity in two distinct NF-κB pathways: "canonical" (left panel) and "non-canonical" (right panel) are schematically shown.

E. Precursor Inhibitors of NF-κB: kappaBsomes

p105 and p100 can generate p50 and p52, respectively. However, they cannot be completely processed. A large fraction of these precursor proteins must remain unprocessed to inhibit of NF-κB proteins including their processed products. Interestingly, both p105/IκBγ and p100/IκBδ use an unusual strategy to inhibit NF-κB. Unlike classical inhibitors such as IκBα which inhibits NF-κB by forming 1:1 complexes, the precursor inhibitors inhibit NF-κB by forming large assembles. These complexes are referred to as the kappaBsomes (κBsomes) (Figure 1.6). A single κBsome complex can contain multiple NF-κB subunits. The only distinction between p105 and p100-centric κBsomes is the presence of p52 and RelB in p100-centric κBsomes but not in p105-centric κBsomes. p100-centric κBsomes thus contain all NF-κB subunits. Perhaps the broad inhibitory capacity that is characteristic of p100/IκBδ makes this inhibitor highly important. Consequently, the processing of p100 is tightly regulated. Inducers of both canonical and non-canonical signaling activate the expression of p100. The p100-containing κBsomes generated during canonical signaling squelch newly synthesized NF-κB. This results in enhanced amounts of the p100: NF-κB complex that in turn limits canonical signaling (Novack et al., 2003; Almaden et al. 2014).

κBsomes were discovered in our laboratory. Through the work of our previous members, we have uncovered some characteristics of these inhibitors and mechanism of processing. Nevertheless, there are several unanswered questions that remains to be addressed. My thesis deals with the understanding of how p100 functions as an inhibitor of NF-κB.

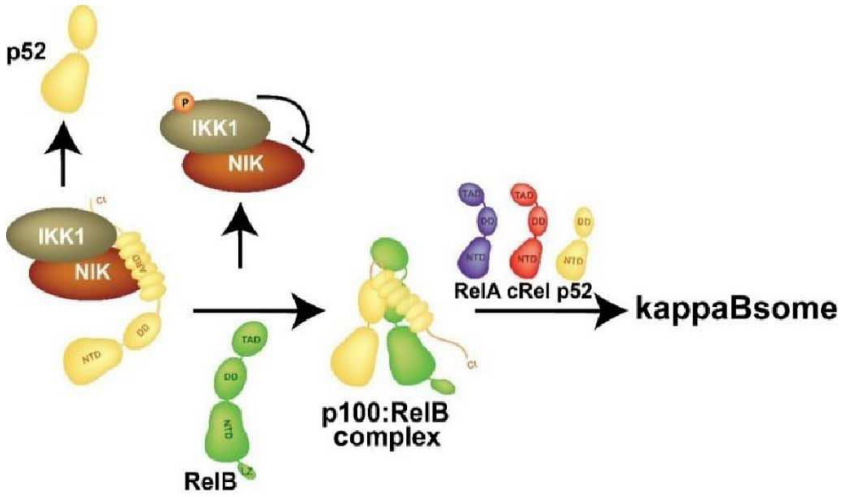

Figure 1.5. Model of kappaBsome formation.
A model depicting the formation of p100-centric κBsome by p100:RelB complex further associating with other NF-kB subunits. (Fusco et al., 2016)

F. PRMT5:MEP50 Complex Might be Required for p100-mediated NF-κB Inhibition

The structure and composition of κBsomes in the non-canonical pathway remain unclear since *in vivo* p100-containg complex is stable, yet *in vitro* assembled complex of κBsome is not. Previous studies done in the Ghosh lab show that RelB is a critical component of the p100-containing κBsome as the characteristic high molecular weight complexes do not form in its absence (Fusco et al., 2016). Yet, other cellular component(s) can be a critical part of κBsomes, and interactions between these components and RelB:p100 within the κBsomes can explain the molecular basis for NF-κB inhibition by p100.

Previous mass spectrometry analysis of the affinity purified κBsome complex isolated from HEK 293 cells indicated the presence of PRMT5 (protein arginine methyltransferase 5). *In vivo* assays also showed that PRMT5 and MEP50 can be pulled down with flag-p100. Thus, PRMT5 and MEP50 may be a component of p100-centric κBsomes

PRMT5 belongs to the S-adenosyl methionine (SAM) dependent methyl-transferase enzymes. These enzymes are responsible for the transfer of a methyl group from SAM to the arginine side-chains of different proteins (Bedford et al.,2009). The methylosome protein 50 (MEP50/WDR77) is an androgen receptor co-activator that forms a stable complex with PRMT5. It is primarily responsible for facilitating substrate binding of PRMT5 (Friesen et al., 2002). A recent crystal structure of human PRMT5:MEP50 is revealed as a hetero-octamer when bound to target H4 (Antonysamy et al., 2012). PRMT5 was also reported to methylate Arg30 of RelA and this modification was shown to be important for nearly 90% of genes activated by RelA when cells are induced with IL-1b,

one of the many cytokines that induces NF-κB activity (Wei et al., 2013), which correlates PRMT5 with NF-κB proteins.

G. Focus of Study

κBsome complexes were discovered in our laboratory in 2009 and since then efforts were made to purify these complexes for structural characterizations. However, in spite of trials by several past members, stable homogeneous complexes could not be produced. This led to the hypothesis that other proteins *in vivo* associate with κBsome to maintain their stabilities. Accordingly, PRMT5 was identified using the pull-down approach from mammalian cell extracts followed by mass-spectrometry. PRMT5 is known to interact with variety of proteins, but it primarily associates with MEP50. It appears that these proteins are stable cognate partners.

The focus of my project is to investigate whether PRMT5 and its partner MEP50 stoichiometrically associate with p100 and the other NF-κB subunits in the κBsome complex. Two important questions I ask are 1) Does the PRMT5:MEP50 complex associate with the p100-centric κBsome complex *in vitro*? 2) What is the role of the PRMT5:MEP50 complex in the regulation of p100 processing? To address these questions, I plan to 1) express and purify the components of the κBsome complex in both truncated and full-length versions in *E*. coli or Sf9 baculovirus expression systems as necessary; 2) clone and express PRMT5 and MEP50 in Sf9 baculovirus expression system and purify the PRMT5:MEP50 complex; 3) test assembly of κBsome and PRMT5 complexes *in vitro*; 4) test if PRMT5:MEP50 complex alters phosphorylation of p100 by NIK:IKK1. To accomplish the last goal, I will purify NIK:IKK1 from baculovirus infected Sf9 cells. All proteins are expressed as poly histidine fusion proteins.

II. Materials and Methods

A. Insect Cell Protocols

1.Preparation of pFastBac plasmid and bacmid

Full length human PRMT5 was amplified by PCR from a commercial mammalian plasmid and cloned into pFastBac HTa (Invitrogen) vector between the restriction sites of EcoRI and XhoI (New England Biolabs). Full length human MEP50 was amplified by PCR from cDNA of 293T cells (from lab member Yidan Li) and cloned into pFastBac HTa vector between the restriction sites of EcoRI and SalI. The digested PCR products and vectors were ligated using T4 DNA ligase (New England Biolabs) and transformed into DH5α *E*. coli strain. Colonies obtained were screened for successful insertion of the PCR product by restriction analysis and sequencing. The primers for PRMT5 and MEP50 amplification are given below with the co-responding restriction site.

hPRMT5(1-667) Forward (EcoRI) 5’ - CCG GAA TTC ATG GCG GCG ATG GCG GTC GG - 3’

hPRMT5(1-667) Reverse (XhoI) 5’ - CCG CTC GAG CTA GAG GCC AAT GGT ATA TGA GCG - 3’

hMEP50 (2-342) Forward (EcoRI) 5’ - CCG GAA TTC CGG AAG GAA ACC CCA CCC - 3’

hMEP50 (2-342) Reverse (SalI) 5’ - A CGC GTC GAC CTA CTC AGT AAC ACT TGC AGG - 3’

pFastBac HTa plasmid constructs of PRMT5, MEP50, and RelB (from former lab member Zhihua Tao) were introduced into DH10Bac *E*. coli strain (Invitrogen). DH10Bac cells support recombination of transfer plasmid with bacmid DNA. Transformed DH10Bac cells were plated onto SOC agarose plate containing kanamycin, gentamicin, tetracycline,

Blue-gal, and IPTG and screened using blue-white colony after 48 hours incubation. The white colonies were then struck onto a fresh SOC agarose plate containing kanamycin, gentamicin, tetracycline, Blue-gal, and IPTG to confirm phenotype. Bacmid DNA was isolated from DH10Bac using Miniprep kit (Biopioneer) and used to transfect Sf9 insect cells (Invitrogen) for viral amplification described below.

2. Sf9 viral amplification

The P1 viral stocks of full length human PRMT5, human MEP50, mouse RelB, human RelA, and human p100 were created by transfecting Sf9 cells at 0.8 million cells/mL on 6-well plates with Cellfectin (Invitrogen), unsupplemented SF-900 media (Lonza), and dilute bacmid DNAs (p100 from Zhihua and RelA from James Kadonaga's Lab) following the Bac-to-Bac Invitrogen protocol. The supernatant was collected 96 hours post-transfection. A P2 viral stock was created by amplifying the viral stock through another infection of Sf9 cells at 1 million cells/mL in 6-well plates and collecting the supernatant after 96 hours. From this stock, the infection was optimized through several dilutions and cell lysis was analyzed using Western Blots with the anti-His antibody (Bio Bharati). The best expression ratio was chosen as P3 viral stock for larger scale protein expression described below.

3. Sf9 protein expression

Sf9 cells in suspension culture were infected with the P3 viral stock for 72 hours at 175rpm, 27 °C. The cells were collected and spun down at 3000 rpm for 25 min at 4°C. The supernatant was aspirated and the pellet was resuspended with 10 pellet volumes of

DPBS (Gibco) and spun down again at 3000 rpm for 10 min at 4°C. The pellet was stored in -80°C for further purification.

4. Sf9 cell lysis

Sf9 cell pellet were resuspended in 40mM Tris HCl pH 8.0, 200 mM NaCl, 10% glycerol, 0.05% TritonX-100, 5mM β-Mercaptoethanol (BME), 1mM PMSF and 0.1X Protease Inhibitor Cocktail (Sigma Aldrich). The cells were lysed by sonication and inclusion bodies were removed from the lysate by centrifugation at 13,000 rpm, 4 °C for 25 minutes. The soluble lysate was used in nickel purification described below.

B. *E*. coli Cell Protocols

1. Plasmid DNA extraction.

Plasmids with Mouse RelB 1-415 and Human RelA 1-325 constructed by previous lab members were transformed into *E*. coli DH5α on LB agarose plate with 100μg/mL ampicillin. 5 mL of bacterial culture was grown overnight from a single colony. Plasmid DNA was extracted and screened for efficient expression by small scale *E*. coli expression and Ni/SP pull down.

2. *E*. coli protein expression

Purified plasmid DNA was used to transform the Rosetta *E*. coli strain. Transformed bacterial cells were cultured in 2L LB media with 100 μg/ml ampicillin and grown at 37 °C to OD600 of approximately 0.5. The cells were then induced with 0.3 mM Isopropyl β-D-1-thiogalactopyranoside (IPTG) for 16 h at approximately 24 °C with vigorous stirring to ensure sufficient aeration. Cells were pelleted by centrifugation at 3000 rpm for 30 min and the pellet was stored in -80°C for further purification.

3. *E*. coli cell lysis

RelB-transformed Rosetta *E*. coli cells were lysed by sonication in 20mM Tris HCl pH 7.5, 1000 mM NaCl, 10% glycerol, 0.5mM PMSF and 0.1X PIC. Insoluble material was removed from the lysate by centrifugation at 13,000 rpm for 40 minutes. The soluble lysate was further purified by Nickel column chromatography described below.

RelA-transformed Rosetta *E*. coli cells were lysed by sonication in 25mM 2-ethanesulfonic acid (MES) pH 6.5, 50mM NaCl, 0.5mM EDTA, 0.5mM PMSF, 10mM

BME, and 1mM Benzamidine. Supernatant was obtained by centrifugation at 13,000 rpm, 4 °C for 30 minutes and mixed with 1/9 volume of 10% streptomycin for 20 minutes at 4 °C. The mixture was further separated by centrifugation at 13,000 rpm for another 30 minutes. The soluble lysate was used in SP purification described in the following subsection.

C. Protein Purification Protocols

1. Nickel column chromatography

The soluble lysate was loaded onto a gravity flow Nickel column (Ni-NTA resin from Bio Bharati). and washed with 30 mM Imidazole in cell lysis buffer without PMSF and PIC 10 column volumes. The protein was eluted with 15 mL of 250 mM Imidazole in cell lysis buffer without PMSF and PIC. Peak fractions were identified through Bradford Assays (Bio-Rad) and confirmed by 10% SDS-PAGE prior to pooling together.

2. Anion exchange column chromatography

Desalted cell lysate or purified protein/protein complex was loaded onto a MonoQ 5/50 GL (GE Healthcare) or MiniQ 4.6/50 PE (GE Healthcare) column in a 50mM NaCl buffer and eluted with a 50mM to 1M NaCl gradient. Peak fractions were confirmed by 10% SDS-PAGE prior to pooling together. Pooled protein was concentrated through an Amicon Ultra-4 (EMD Millipore) concentrator used in further purification or other assays.

3. Cation exchange column chromatography

Desalted RelA *E.* coli cell lysate was loaded onto a MonoS 5/50 GL (GE Healthcare) column in a 50mM NaCl buffer and eluted with a 50mM to 1M NaCl gradient. Peak fractions were confirmed by 10% SDS-PAGE prior to pooling. Pooled protein was flash frozen in -80°C and used in further purification or other assays.

4. Size exclusion column chromatography

Purified protein/protein complex was loaded onto a Superose 6 Increase 5/150 GL or 10/300 GL (GE Healthcare) column in a buffer of 40 mM Tris-HCl pH 8.0, 250 mM NaCl, 10% Glycerol, 0.5mM EDTA, 2mM BME, and 0.5mM DTT. Peak fractions were analyzed by 10% SDS-PAGE to confirm the purity of the protein then pooled and flash frozen. Protein was concentrated to at least 1.0 mg/ml as determined by Bradford assay.

D. Western Blot

For detection of human RelA, mouse RelB, human p100/p52, and human PRMT5 by western blotting, rabbit polyclonal RelA antibody (sc372), RelB antibody (sc226) from Santa Cruz Biotechnology, p100/p52 (#1495) rabbit antisera gifted from N. Rice (NIH, Bethesda, MD), and rabbit polyclonal PRMT5 antibody (07-405) from EMD Millipore were used. The protein was loaded and resolved into a 10% SDS-PAGE gel and then transferred onto a PVDF membrane. The membrane was blocked with 0.2% I-Block (Thermo Fisher) before incubating in corresponding primary antibody for 16 hours at 4 °C. The membrane was then incubated with the HRP-conjugated secondary rabbit antibody (Bio Bharati) and developed with 10mL ECL buffer (0.1 mM Tris 8.6, 25 µL p-coumaric acid, 55 µL luminol, and 6µL H_2O_2).

E. *In vitro* assays

1. PRMT5 methylation assay

In vitro methylation assays were conducted in 40 µL reactions using 1.2 µg of purified PRMT5: MEP50 (human full-length PRMT5 and MEP50 from baculovirus expression system) with or without purified substrate (4 µg), and a reaction buffer at a working concentration of 25mM HEPES pH 7.6, 5mM $MgCl_2$, 100mM NaCl, 2.5mM DTT, and 20uM SAM. The mixture was incubated at 37 °C for 90 minutes. After 5, 20, 45, and 90 minutes, 5uL of mixture was aliquoted and 7 µL of 4X SDS sample buffer was added to quench the reaction. A total 12 µL of the mixture was loaded and resolved into a 10% SDS-PAGE gel. The gel was subsequently stained with Coomassie staining.

2. NIK:IKK kinase assay

In vitro kinase assays were conducted in 20 µL reactions using purified NIK:IKK1 (NIK 326-947 and IKK1 S176E/S180E 1-667 from baculovirus expression system) with or without purified substrate(s), and a reaction buffer at a working concentration of 10mM Tris-HCl pH 7.5, 4mM $MgCl_2$, 20mM NaCl, and 1mM DTT. To these reactions, 0.5 µCi of γ-32P ATP (Perkin Elmer) was added, mixed, and incubated at room temperature for 45 minutes. After incubation, 8 µL of 4X Laemmli buffer was added to quench the reaction and 10 µL of the mixture was loaded and resolved into a 10% SDS-PAGE gel. The gel was subsequently exposed to autoradiography film (Denville Scientific) overnight for approximately 12-16 hours prior to developing.

III. Results

A. Cloning and expression of NF-κB proteins in *E*. coli cells

NF-κB protein and its precursor p100 was initially purified separately from *E*. coli or insect cells. Truncated RelB and RelA without TAD were previously shown to be able to be purified from *E*. coli soluble cell lysate with better stability. I purified a large amount of RelA 1-325 and RelB 1-415and used for proceeding attempts to form κBsome complex with baculovirus expressed p100 and PRMT5:MEP50 (Figure 2.1).

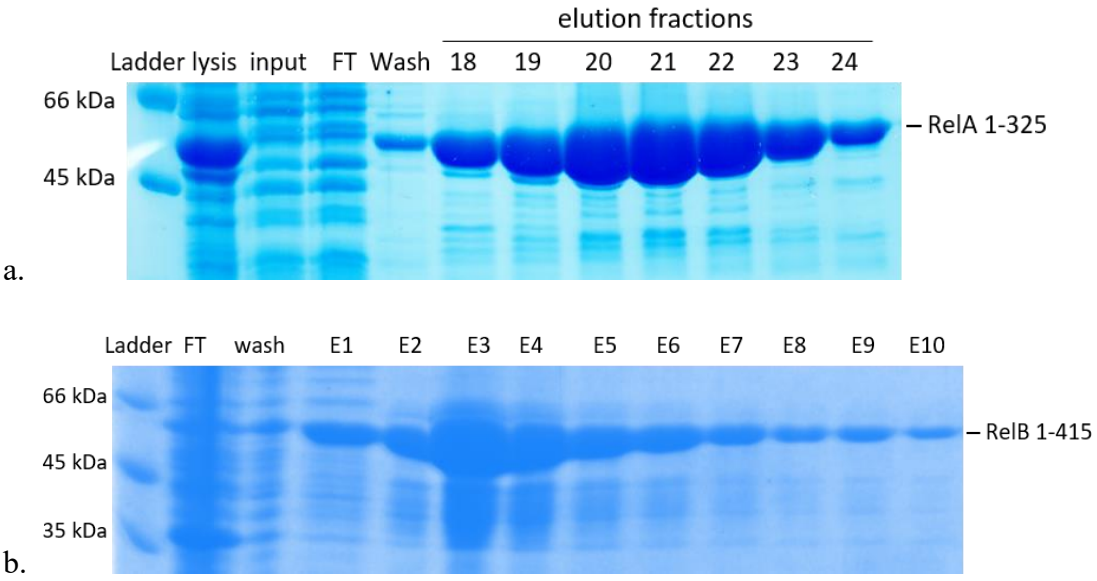

Figure 2.1. Purification of truncated NF-κB proteins from E. coli expression system. RelA 1-325 was purified by SP cation exchange column chromatography (a) and RelB 1-415 was purified by Ni affinity column chromatography (b). Both proteins were and detected by Coomassie stained. SDS-PAGE.

B. Cloning and Expression of NF-κB Proteins in Sf9 cells

Two full length NF-κB proteins (RelA and RelB) and the NF-κB precursor p100 were used to form a complex with PRMT5:MEP50. Since *E*. coli expression of p100 and NF-κB proteins lacks certain post-translational modification which may play a critical role in its activity and protein folding, RelA, RelB, and p100 were each cloned into pFastBac vector and overexpressed in Sf9 cells. Since preliminary results show that *in vitro* assembly of the complex using separately purified protein was not successful, I altered my strategy to co-infect all proteins in Sf9 cells to potentially promote the protein complex formation in cells. After co-infection, I purified the complex through one batch of Ni-NTA purification, which is described below.

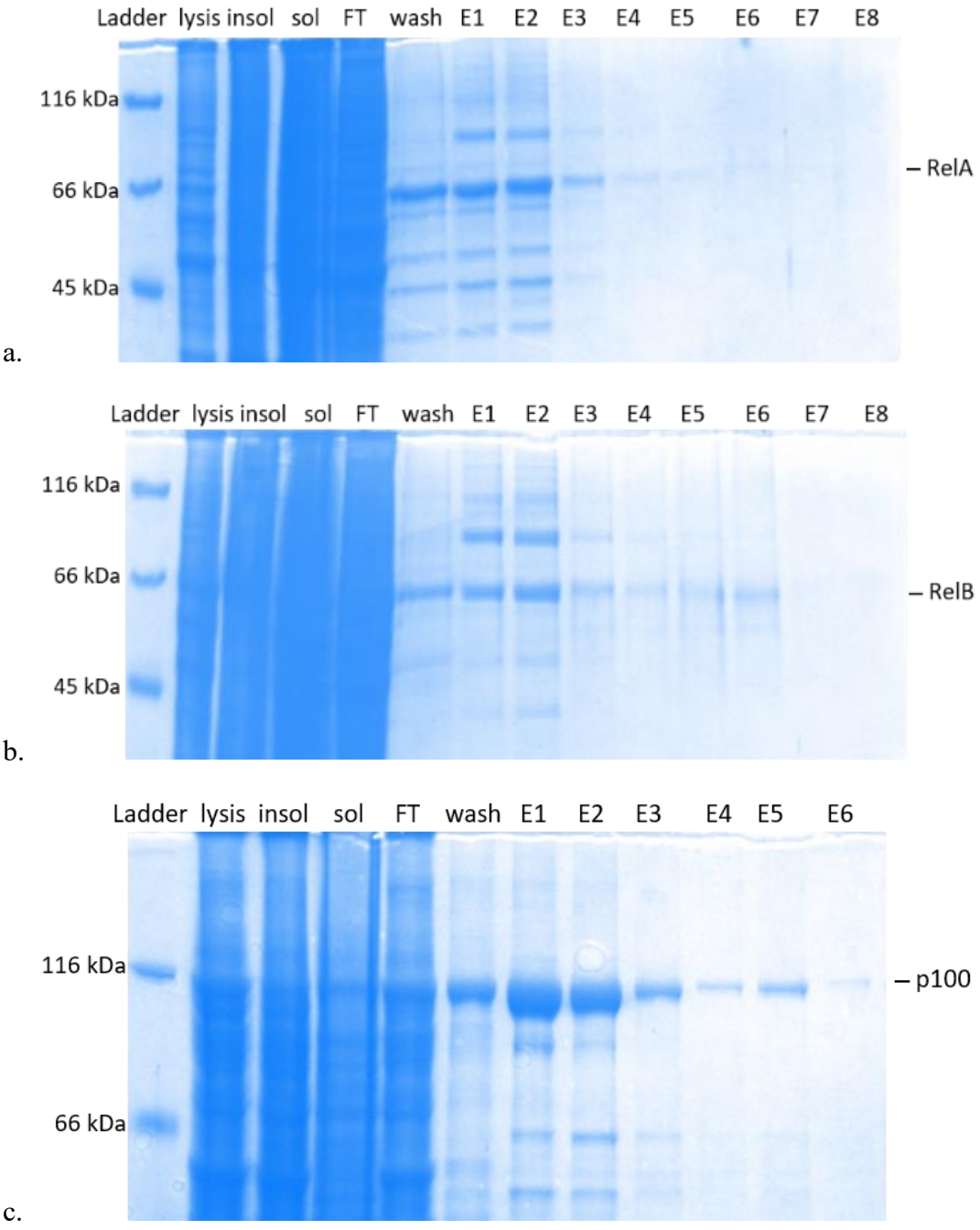

Figure 2.2. Purification of full length p100 and NF-κB proteins from Sf9 baculovirus expressing system.
RelA (a), RelB (b) and p100 (c) were purified by Ni affinity column chromatography and detected by Coomassie stained SDS-PAGE.

C. Cloning and Expression of PRMT5 and MEP50 Proteins in Sf9 cells

PRMT5 can be only expressed and purified from baculovirus infected cells since the bacterially expressed protein is not functional (Emtage et al., 2012). I cloned PRMT5 into a poly his-tagged baculovirus expression plasmid, infected a Sf9 cell suspension culture with the baculovirus, and purified PRMT5 through a Ni-NTA gravity column (Figure 2.3a).

However, the purification was not fully successful since the expression efficiency and stability of this baculovirus expressed PRMT5 was low. Low yield severely affected its ability to form the complex (described below). Previous studies showed that PRMT5 always forms high molecular weight protein complexes that invariably contain the methylosome protein 50 (MEP50) (Emtage et al., 2012; Shechter et al., 2013). Thus, I then sought to co-express PRMT5 and MEP50 in efforts to increase the expression efficiency and protein stability. MEP50 was cloned from cDNA of 293T cells into a poly His-tagged baculovirus expressing plasmid. However, MEP50 by itself was not expressed in the baculovirus system (Figure 2.3b). Thus, I co-infected Sf9 cells with PRMT5 baculovirus. PRMT5 and MEP50 were purified together through Ni-NTA gravity column (Figure 2.3c). Co-infection and co-purification of PRMT5 and MEP50 allowed formation of a complex in the following purification steps to test the strength and stability of this complex. This co-infection strategy also allowed us to test the catalytic activity of the complex through methylation assay on truncated RelA with substrate SAM (Figure 2.3d).

Since p100 and PRMT5 were the first successfully expressed and purified, I attempted to *in vitro* assemble the κBsome complex using truncated RelA and RelB purified from *E*. coli cells (described above), and p100 and PRMT5 from baculovirus-

expressed Sf9 cells. The size exclusion chromatography fractions on SDS-PAGE indicated that PRMT5 by itself did not associate with RelB:p100, whereas we still could not get complex higher than 600 kDa (Figure 2.3e). This preliminary result further confirmed that MEP50 might be required for complex assembly.

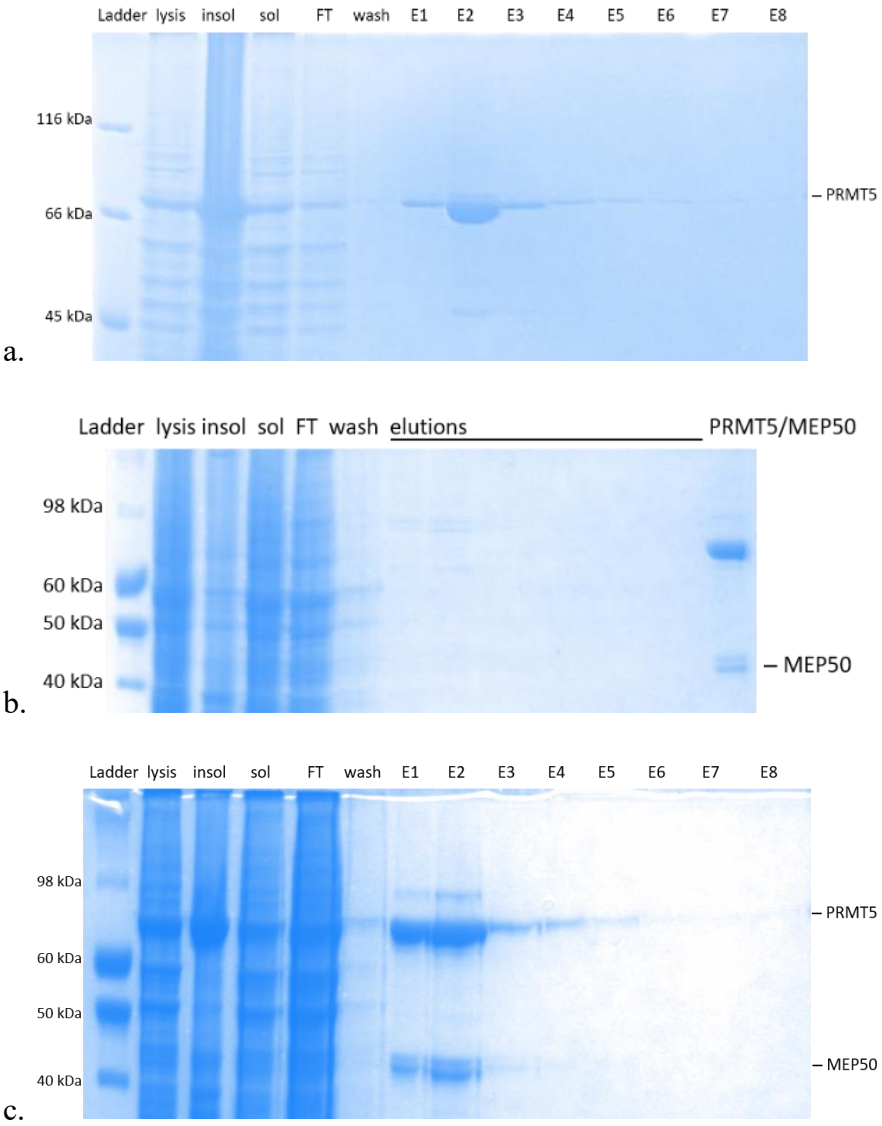

Figure 2.3. Purification of PRMT5 and MEP50 from Sf9 expressing system.
a) Coomassie stained SDS-PAGE of Ni-NTA purified PRMT5 (lane E2).
b) Coomassie stained SDS-PAGE showed *apo* MEP50 could not be expressed.
c) Coomassie stained SDS-PAGE of Ni-NTA purified co-expressing PRMT5 and MEP50 (lane E1-5).

d.

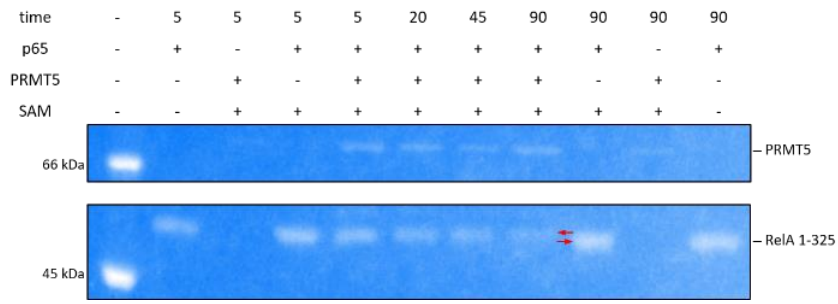

e.

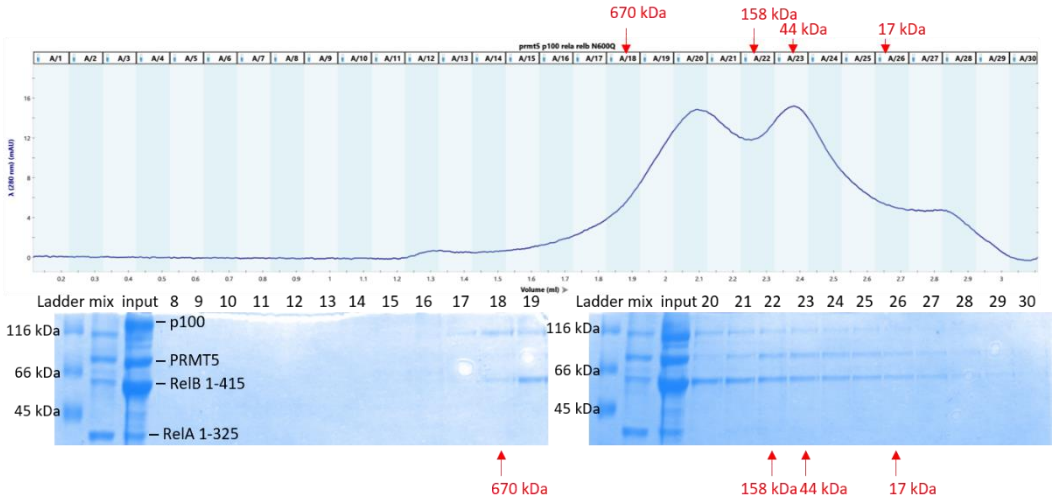

Figure 2.3. (continue) Purification of PRMT5 and MEP50 from Sf9 baculovirus expressing system.

d) Methylation assay of PRMT5:MEP50 on RelA 1-325. Red arrows showed the shift on migration of methylated vs. unmethylated RelA.

e) in vitro assembly of p100, PRMT5, RelB 1-415, and RelA 1-325 analyzed by gel filtration chromatography on Superpose 6 column. A280 was plotted against retention volume (top). The resulting fractions and input samples were analyzed by SDS-PAGE and Coomassie staining (bottom).

D. Purification of κBsome

p100, RelB, RelA, PRMT5, and MEP50 were co-infected in Sf9 cell to ensure the expression efficiency and protein stability. The first attempt of co-expression applied the same virus to cell ratio of 1/100 (Table 2.1 Trial 1) and the result showed NF-κB proteins (RelA and/or RelB) were expressed in low level compared to PRMT5 (Figure 2.4a). Neverless, I was still able to see the co-elution of p100 and PRMT5:MEP50 on size exclusion chromatography (Figure 2.4b) and the following miniQ (anion exchange chromatography) elution fractions (#28-31) (Figure 2.4c). This provided a hint that p100:NF-kB associates with PRMT5:MEP50.

Different virus dilutions were optimized through small scale Ni-NTA purification to ensure the near equivalent expression of all proteins (Figure 2.5a top and Table 2.1). Large scale Sf9 co-infection with MOI confirmed from small scale purification was used for expression of all five proteins. p100, RelB, RelA, PRMT5, and MEP50 were all His-tagged and together purified from 700mL soluble Sf9 cell lysate in one-step of Ni-NTA column chromatography (STEP-1) (Figure 2.5a bottom). The purified protein mix was loaded on a mono-Q column for separation of complex with similar charges from non-participating proteins (STEP-2). Three protein peaks on the chromatogram as well as SDS-PAGE were observed (Figure 2.5b). Fraction #10-11 contained excess RelB/RelA; fraction #13-14 showed a nearly equal amount of p100 and RelB/RelA with no presence of MEP50; and fraction #15-19 may contain two merged peaks: one for all five proteins in stoichiometric amount (#15-18 or 19) and one for excess PRMT5:MEP50 (#16-18).

The pooled fraction #16-19 were further loaded on gel filtration column for further separation (STEP-3) (Figure 2.5c). Interestingly, although only one peak on gel filtration

chromatography was observed, fractions #25-40 show multiple protein compositions (Figure 2.5c). Fraction #24-28, which is in the ideal high molecular weight range, showed a nearly equal amount of all proteins, whereas in Fraction #29-31 contained lesser amounts of the kBsome associated with the PRMT5:MEP50 complex. Fractions after #32 showed an increasing amount of PRMT5:MEP50 and decreasing amount of p100. Three pools were made and two of them were loaded on a mini-Q column separately to further confirm their stability and compositions (Figure 2.5d).

The pools of gel filtration fractions #29-31 and #34-36 were further purified through a miniQ anion exchange column (STEP-4). Through chromatography of both runs, only one peak around fraction #13-15 was observed. However, the SDS-PAGE of fractions indicated that these two complexes had different protein compositions (Figure 2.5e). MiniQ elution from the first gel filtration fraction pool (#29-31) had little amount of p100 (Figure 2.5e top). In addition, p100 completely disappeared from the miniQ elution of the second pool (#34-36) (Figure 2.5e bottom).

a.

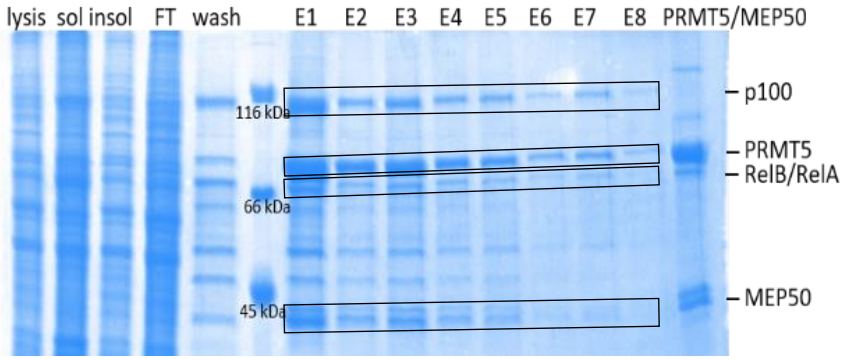

b.

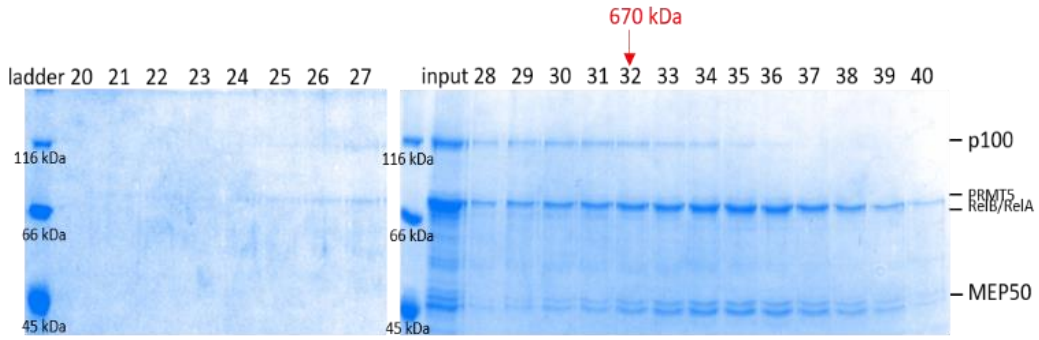

c.

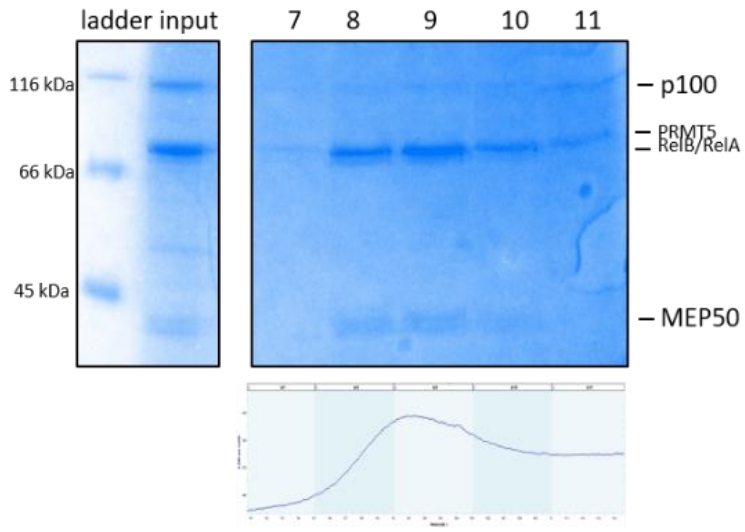

Figure 2.4. Purification of co-expressing five proteins in the same virus:cell ratio.
a) Coomassie stained SDS-PAGE of Ni-NTA purified five proteins.
b) Coomassie stained SDS-PAGE of gel filtration fractions by Superose 6.
c) Coomassie stained SDS-PAGE of miniQ fractions #7-11 with input (top) and corresponding A280 chromatogram.

Table 2.1. Virus to cell ratio of five proteins.
multiplicity of infection (MOI) was altered by changing the ratio number of cells to virus. 1/x stands for virus volume was 1/x mL of culture volume, cell density of culture when infecting was always controlled at $1*10^6$/mL.

Baculovirus	Trial 1	Condition 1	Condition 2
p100	1/100	1/100	1/50
RelB	1/100	1/100	1/100
RelA	1/100	1/100	1/100
PRMT5	1/100	1/200	1/125
MEP50	1/100	1/200	1/125

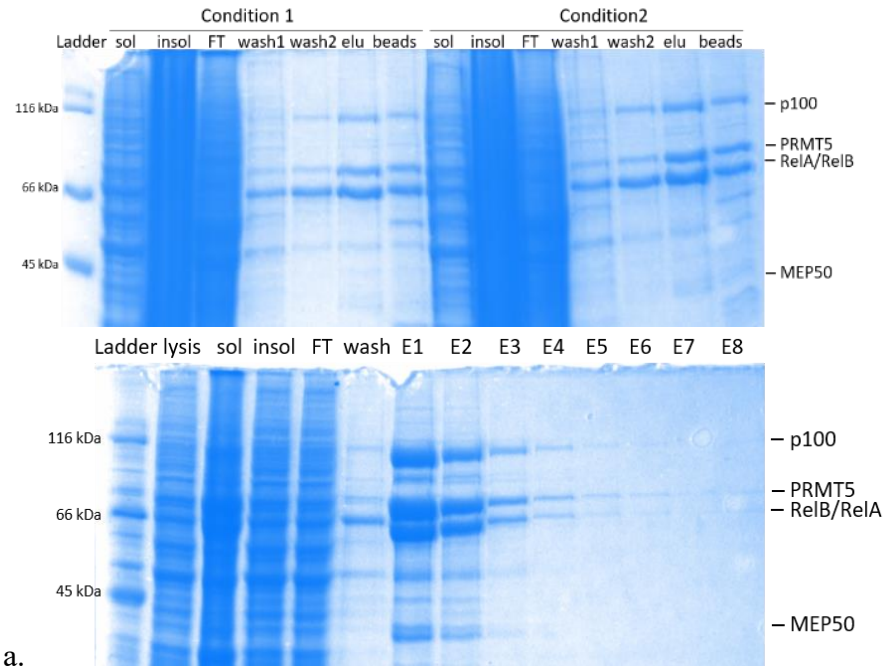

a.

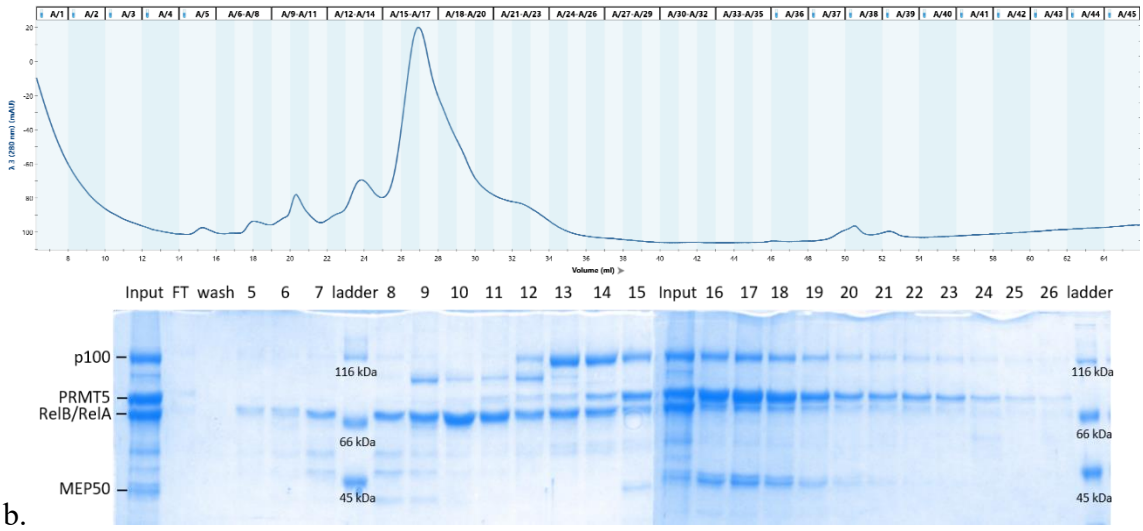

b.

Figure 2.5. Four-step purifications of co-expressing five proteins.
a) Coomassie stained SDS-PAGE of Ni-NTA purified five proteins in small-scale MOI optimization (left) and STEP-1 large-scale purification (right).
b) A280 chromatogram (top) and corresponding Coomassie stained SDS-PAGE (bottom) of STEP-2 anion exchange column chromatography fractions by MonoQ.

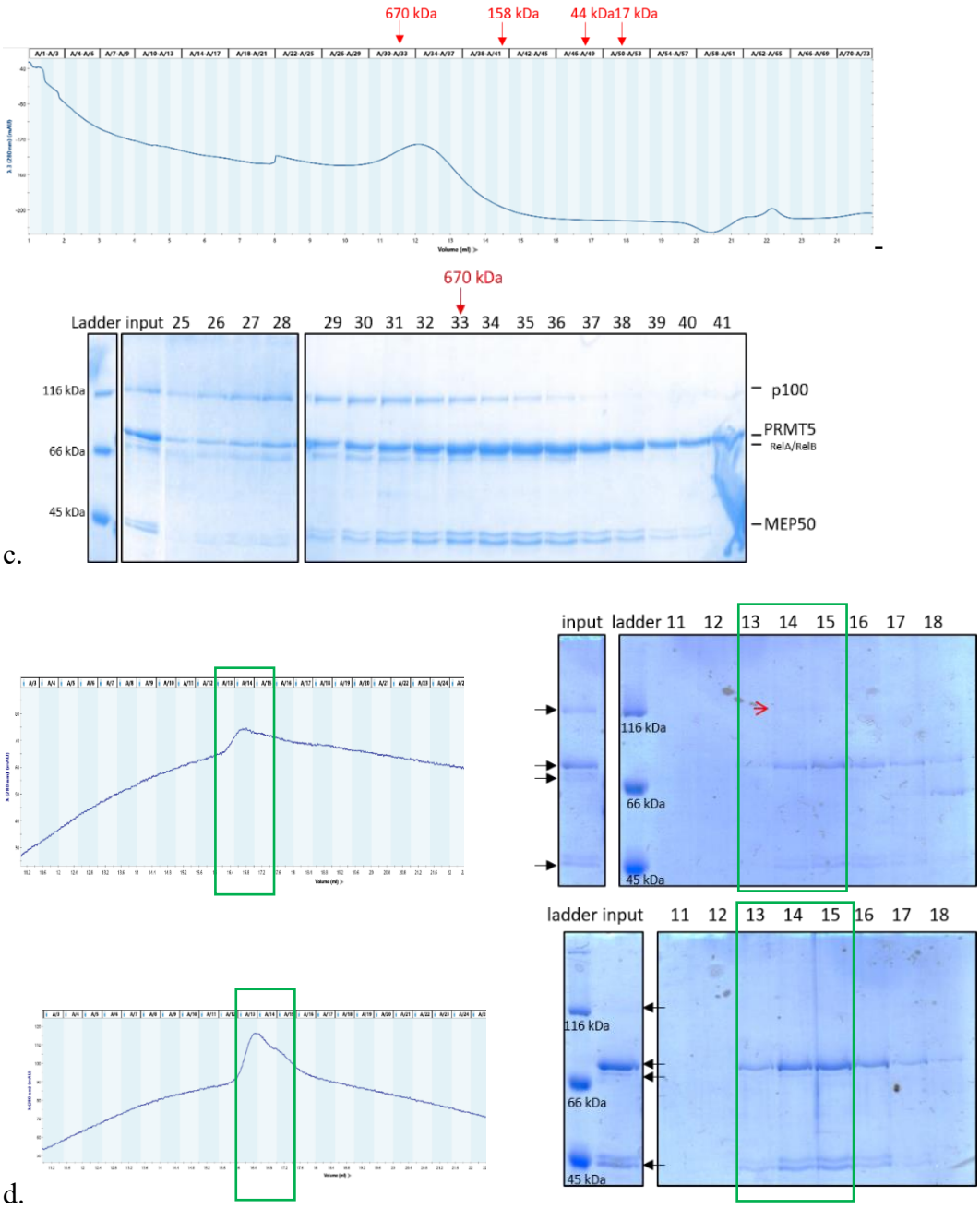

Figure 2.5.(continue) Four-step purifications of co-expressing five proteins.
c) A280 chromatogram (top) and corresponding Coomassie stained SDS-PAGE (bottom) of STEP- 3 size exclusion column chromatography fractions by Superose 6.
d) top: A280 chromatogram (left) and corresponding Coomassie stained SDS-PAGE (right) of STEP-4 anion exchange column chromatography fractions running STEP-3 pool of #29-31; bottom: A280 chromatogram (left) and corresponding Coomassie stained SDS-PAGE (right) of STEP-4 anion exchange column chromatography fractions running STEP-3 pool of #34-36.

E. Composition of the κBsome Complex

The fractions from each purification step of co-expressed kBsome was analyzed with immunoblot to identify the components of the complex. Small amount of pooled fractions of Ni-NTA column, gel filtration column, and both anion exchange column chromatography was blotted against five protein-specific antibodies. Separately purified proteins and complexes were used as positive controls for immunoblot. The amount of protein is not equivalent throughout the fractions but their presence and a relative trend of protein concentration were able to be observed.

The western blot result indicated that p100, RelA, RelB, and PRMT5 all persisted throughout four steps of protein purification (Figure 2.6). Since previous results showed that MEP50 always forms a strong complex with PRMT5, we can conclude that MEP50 is also present in all steps of purification. These immunoblot results were consistent with previous results of Coomassie staining SDS-PAGE of purification fractions (Figure 2.5) and indicate the association between PRMT5 complex and kBsome complex.

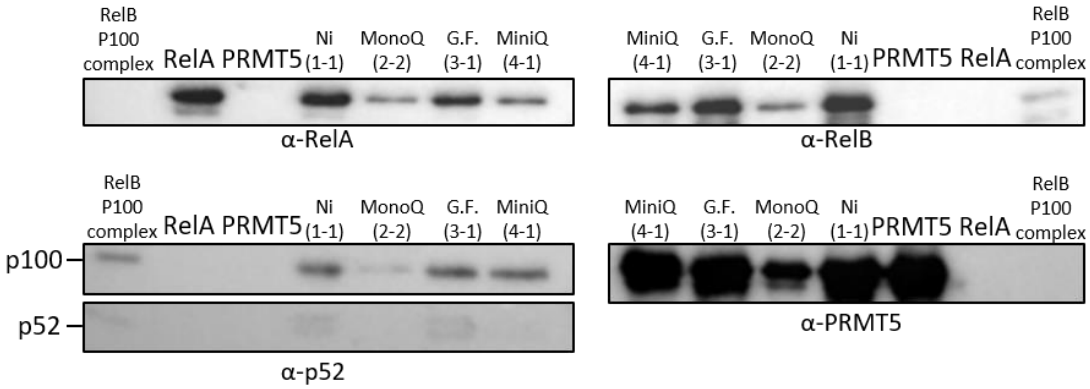

Figure 2.6. Identification of kBsome complex components.
Western blot analysis of fractions from all steps of kBsome purification experiments with separately purified positive control proteins. (1-1) was obtained from STEP-1 pooled Ni purification fractions. (2-2) was obtained from STEP-2 pooled MonoQ purification fraction #16-19. (3-1) was obtained from STEP-3 pooled gel filtration purification fractions #24-28. (4-1) was obtained from STEP-4 pooled MiniQ gel filtration purification fractions.

F. PRMT5:MEP50 Affects p100 Processing

In non-canonical signaling, NIK:IKK1 complex is known as the kinase to phosphorylate p100 and thereby activating non-canonical signaling pathway *in vivo*. Thus, we tested if the interaction between PRMT5:MEP50 complex and the kBsome complexes would affect phosphorylation of p100. NIK 326-947 and IKK1 EE (S176E/S180E as amino acid substituted dominant positive) 1-667 was co-expressed in Sf9 cell and used as the kinase for this assay (Figure 2.7a).

The results revealed that *apo* p100 can be phosphorylated by NIK:IKK1. However, p100 phosphorylation was inhibited upon addition of other proteins. RelB alone could substantially inhibit p100 phosphorylation, yet RelA could only inhibit in an insignificant level. PRMT5:MEP50 complex alone also partially inhibited p100 phosphorylation, and the inhibition effect can accumulate by mixing various interacting proteins in different combinations (Figure 2.7b).

On the other hand, p100 in the purified complex from step 3 of gel filtration using co-expressed five-member complex could not be phosphorylated at all (Figure 2.7c.). This result was consistent with the mixing assay and further confirmed that p100 phosphorylation was majorly inhibited by RelB and partially by PRMT5:MEP50.

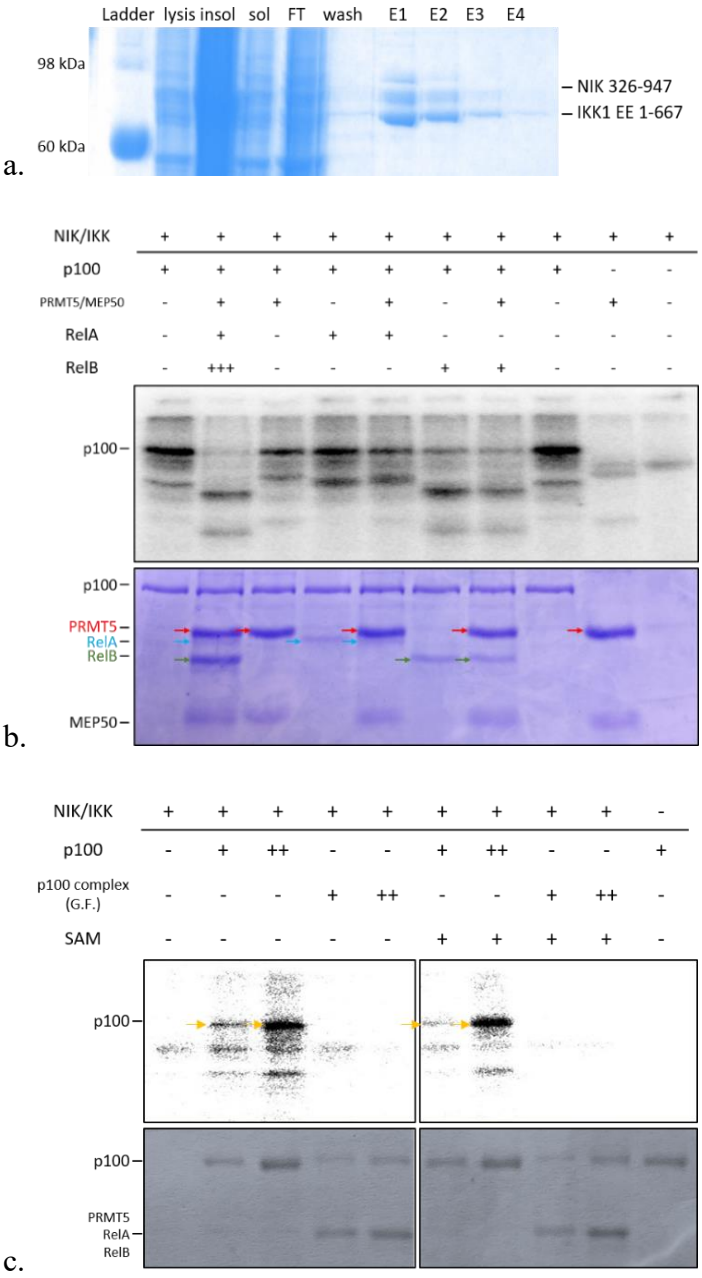

Figure 2.7. p100 and p100 complex phosphorylated by NIK:IKK1.
a) Coomassie stained SDS-PAGE of Ni-NTA purified baculovirus expressing NIK:IKK1 (lane E1-E2).
b) *in vitro* kinase assay by NIK:IKK1 on free p100 and p100 mixing with various interacting proteins.
c) *in vitro* kinase assay by NIK:IKK1 on free p100 and p100 complex purified from STEP-3 (see Figure 2.5c).

IV. Discussion

A. *In vitro* Interaction Between p100 and RelB

Previous data showed that RelB is an integral part of the p100-κBsome and that the high molecular weight p100-centric kBsome complex in the cell only exists in presence of RelB (Fusco et al., 2016). In my preliminary experiments, I attempted to form the RelB-p100 complex by *in vitro* assembly as well as by co-expressing RelB and p100 in baculovirus infected Sf9 cells. Although p100 and RelB associates each other, during purification of the p100:RelB complex in Sf9 cells, RelB disappears from the fractions containing p100. Similarly, mixing of pure p100 with bacterially expressed truncated RelB (1-415) revealed their association, but the complex eluted as an ~400 kDa complex. These observations are consistent with previous observations in the lab. Strikingly, p100 and RelB remain associated along with other NF-kB proteins in the cell. These results led us to propose the association of kBsome with other factors in cells. Accordingly, PRMT5 was found be associated with p100 but no experiment was performed to support this. I undertook the study to reveal if indeed p100 (kBsome) and PRMT5 interact and if this interaction is functionally important.

B. PRMT5:MEP50 Complex Associates with p100-κBsome *in vitro*

Prior pull down experiments only identified PRMT5 but not its integral partner MEP50. Therefore, I wished to include MEP50 in my study along with PRMT5. To study the *in vitro* interaction, one must obtain large amounts of partner proteins. My goal was to generate each protein in large amounts. Each of these proteins can only be expressed in the baculovirus expression system in their full-length versions. Although some of the viruses expressing some of these proteins were available, I had to make the viruses for the others.

In particular, I put most of my efforts to generate the baculovirus expression systems for PRMT5 and MEP50. cDNA clones of PRMT5 was available in the lab, which I then cloned into a viral expression vector and subsequently generated the virus. MEP50 had to be isolated from total cellular cDNA and cloned into the viral vector. Expression of each protein was initially tested in small scale and the purification was optimized. However, I have shown that mixing the pure proteins was not very suitable for the complex formation.

Thus, I decided to co-express all five proteins (p100, RelA, RelB, PRMT5, and MEP50) in Sf9 cells. Purification of the putative complex(es) was carried out by multiple chromatographic steps. Based on the analysis of the fractions from each purification step, it became clear that at least three complexes existed in the pool: p100 and RelB/RelA formed a separate complex since it mostly devoid of MEP50 (Figure 2.5b, MonoQ-fraction #13-14). All five proteins existed in two other pools. However, their stoichiometry varied. In one of these pools, all component appeared to be present in appropriate ratio (Figure 2.5c, Gel Filtration-fraction #24-28), whereas the other pool contained lesser amounts of kBsome associated with the PRMT5:MEP50 complex (Figure 2.5c, gel filtration-fraction #29-31). In addition, PRMT5:MEP50 also appeared in a separate complex devoid of any kBsome complex (Figure 2.5c, gel filtration-fraction #37-41). If the association between the kBsome and PRMT5:MEP50 were highly stable, then two distinct pools wound not have existed and in the final purification step large amounts of this complex could be isolated. This unusual property of complex formation led us to think that the association between these two complexes (kBsome and PRMT5:MEP50) is dynamic. In this rather dynamic complex, PRMT5:MEP50 might act as a stable structural scaffold which is targeted by the unstable kBsome for binding. The continuous interaction with

PRMT5:MEP50 scaffold might maintain the structural integrity of kBsome. This prevents degradation of RelB which is known to be highly degradation prone. The association between is p100-kBsome and PRMT5:MEP50 complex further confirmed by kinase assay result that PRMT5 partially inhibits p100 phosphorylated by NIK:IKK1.

C. Inhibition of p100 Phosphorylation by RelB/RelA/PRMT5:MEP50

One critical aspect of this dynamic interaction is that if such an interaction is functionally relevant. Therefore, we tested p100 phosphorylation by NIK:IKK1. It is known that these kinases, activated *in vivo* through non-canonical signaling, phosphorylate p100 which is essential for its processing into p52. We found that that whereas free p100 is phosphorylated by these kinases, p100 in the complex is not. By mixing various interacting proteins in different combinations, I further found that RelB alone significantly inhibits p100 phosphorylation, but RelA alone does not. PRMT5:MEP50 complex alone can partially inhibit p100 phosphorylation, which is greatly inhibited in the presence of RelB (Figure 2.7b). These results suggest that PRMT5:MEP50 not only maintains the stability of kBsome, but also maintains its homeostatic repression by preventing aberrant phosphorylation. In cellular terms, prevention of aberrant phosphorylation of p100, hence inhibition of its processing, is extremely important. It is known that uncontrolled processing of p100 into p52 leads to excessive proliferation of cell. At the same time, lack of stable complex formation between the kBsome complex and PRMT5:MEP50 complex might lead to easy separation of this dynamic complex allowing p100 to undergo processing under stimulated condition.

REFERENCES

Antonysamy, S., Bonday, Z., Campbell, R., Doyle, B., Druzina, Z., Gheyi, T., Bomie Han, Louis N. Jungheim, L. N., Qian, Y., Rauch, C., Russell, M., Sauder, J. M., Wasserman, S. R., Weichert, K., Willard, F. S., Zhang, A. and Emtage, S. (2012) Crystal structure of the human PRMT5:MEP50 complex. *Proceedings of the National Academy of Sciences of the United States of America*, 109(44), 17960-17965.

Almaden, J. V., Tsui, R., Liu, Y. C., Birnbaum, H., Shokhirev, M. N., Ngo, K. A., Davis-Turak, J.C., Otero, D., Basak, S., Rickert, R.C. and Hoffmann, A. (2014) A Pathway Switch Directs BAFF Signaling to Distinct NF-κB Transcription Factors in Maturing and Proliferating B Cells. *Cell Reports*, *9*(6), 2098–2111.

Baeuerle, P.A. and Baltimore, D. (1996) NF-κB: ten years after. *Cell*, 87, 13-20.

Baeuerle, P.A. and Henkel, T. (1994) Function and activation of NF-κB in the immune system. *Annual Review of Immunology*, 12, 141-179.

Baldwin, A.S., Jr. (1996) The NF-κB and IκB proteins: new discoveries and insights *Annual Review of Immunology*, 14, 649-683.

Bedford, M.T. and Clarke, S.G. (2009) Protein arginine methylation in mammals: who, what, and why. *Molecular Cell*. 33(1), 1-13.

Bours, V., Villalobos, J., Burd, P.R., Kelly, K. and Siebenlist, U. (1990) Cloning of a mitogen-inducible gene encoding a κB DNA-binding protein with homology to the rel oncogene and to cell-cycle motifs. *Nature*, 348, 76-80.

Chen, F.E., Huang, D.B., Chen, Y.Q. and Ghosh, G. (1998a) Crystal structure of p50/p65 heterodimer of transcription factor NF-κB bound to DNA. *Nature*, 391, 410-413.

Chen, Y.Q., Ghosh, S. and Ghosh, G. (1998b) A novel DNA recognition mode by the NF-κB p65 homodimer. *Nature Structural & Molecular Biology*, 5, 67-73.

Chen, Y.Q., Sengchanthalangsy, L.L., Hackett, A. and Ghosh, G. (2000) NF-κB p65 (RelA) homodimer uses distinct mechanisms to recognize DNA targets. *Structure*, 8, 419-428.

Delhase, M., Hayakawa, M., Chen, Y. and Karin M. (1999) Positive and negative regulation of IκB kinase activity through IKKβ subunit phosphorylation. *Science*, 284, 309-313.

Friesen, W.J., Wyce, A., Paushkin, S., Abel, L., Rappsilber, J., Mann, M. and Dreyfuss, G. (2002) A novel WD repeat protein component of the methylosome binds Sm

proteins. *Journal of Biological Chemistry*, 277(10), 8243-8247.

Fusco, A.J., Savinova, O.V., Talwar, R., Kearns, J.D., Hoffmann, A. and Ghosh G. (2008) Stabilization of RelB requires multidomain interactions with p100/p52. *Journal of Biological Chemistry*, 283, 12324-12332.

Fusco, A.J., Mazumder, A., Wang, V.Y., Tao, Z., Ware, C. and Ghosh, G. (2016) The NF-κB subunit RelB controls p100 processing by competing with the kinases NIK and IKK1 for binding to p100. *Science Signaling*, 9, 447, ra96.

Ghosh, G., van Duyne, G., Ghosh, S. and Sigler, P.B. (1995) Structure of NF-κB p50 homodimer bound to a κB site. *Nature*, 373, 303-310.

Ghosh, S., May, M.J. and Kopp, E.B. (1998) NF-κB and Rel proteins: evolutionarily conserved mediators of immune responses. *Annual Review of Immunology*, 16, 225-260.

Ghosh, S. and Baltimore, D. (1990) Activation in vitro of NF-κB by phosphorylation of its inhibitor IκB. *Nature*, 344, 678-682.

Ghosh, S. and Karin, M. (2002) Missing pieces in the NF-κB puzzle. *Cell*, 109 Supplement 1, S81-96.

Hayden M.S. and Ghosh, S. (2004) Signaling to NF-κB. *Genes and Development*, 18, 2195-2224.

Hoffmann, A., Natoli, G. and Ghosh, G. (2006) Transcriptional regulation via the NF-κB signaling module. *Oncogene*, 25(51), 6706-6716.

Ho, M.-C., Wilczek, C., Bonanno, J. B., Xing, L., Seznec, J., Matsui, T., Carter, L., Onikubo, T., Kumar, R.P., Chan, M.K., Brenowitz, M., Cheng, R.H., Reimer, U., Almo, S.C. and Shechter, D. (2013) Structure of the arginine methyltransferase PRMT5-MEP50 reveals a mechanism for substrate specificity. *PLoS ONE*, 8(2), e57008.

Huxford, T., Huang, D.B., Malek, S. and Ghosh, G. (1998) The crystal structure of the IκB/NF-κB complex reveals mechanisms of NF-κB inactivation. *Cell*, 95, 759–770.

Karin, M. and Ben-Neriah, Y. (2000) Phosphorylation meets ubiquitination: the control of NF-κB activity. *Annual Review of Immunology*, 18, 621-663.

Kieran, M., Blank, V., Logeat, F., Vandekerckhove, J., Lottspeich, F., Le Bail, O., Urban, M.B., Kourilsky, P., Baeuerle, P.A. and Israel, A. (1990) The DNA binding

subunit of NF-κB is identical to factor KBF1 and homologous to the rel oncogene product. *Cell*, 62, 1007-1018.

Lu, T., Yang, M., Huang, D.-B., Wei, H., Ozer, G. H., Ghosh, G. and Stark, G. R. (2013) Role of lysine methylation of NF-κB in differential gene regulation. *Proceedings of the National Academy of Sciences of the United States of America*, *110*(33), 13510–13515.

Novack, D.V., Yin, L., Hagen-Stapleton, A., Schreiber, R.D., Goeddel, D.V., Ross, F.P. and Teitelbaum, S.L. (2003) The IκB function of NF-κB2 p100 controls stimulated osteoclastogenesis. *Journal of Experimental Medicine*, 198, 771-781.

Oeckinghaus, A. and Ghosh, S. (2009) The NF-κB family of transcription factors and its regulation. *Cold Spring Harbor Perspectives in Biology*, 1(4), a000034.

Oeckinghaus, A., Hayden, M.S. and Ghosh, S. (2011) Crosstalk in NF-κB signaling pathways. *Nature Immunology*, 12, 695–708.

Ruben, S.M., Klement, J.F., Coleman, T.A., Maher, M., Chen, C.H. and Rosen C.A. (1992) I-Rel: a novel rel-related protein that inhibits NF-κ B transcriptional activity. *Genes Development*, 6, 745-760.

Ryseck, R.P., Novotny, J. and Bravo R. (1995) Characterization of elements determining the dimerization properties of RelB and p50. *Molecular and Cellular Biology*, 15, 3100-3109.

Schuster, M., Annemann, M., Plaza-Sirvent, C. and Schmitz I. (2013) Atypical IκB proteins-nuclear modulators of NF-κB signaling. *Cell Communication and Signaling*, 11, 23.

Sen, R. and Baltimore, D. (1986) Multiple nuclear factors interact with the immunoglobulin enhancer sequences. *Cell*, 46, 705-716.

Malek, S., Huang, D.B., Huxford, T., Ghosh, S. and Ghosh, G. (2003) X-ray crystal structure of an IκBβ:NF-κB p65 homodimer complex. *Journal of Biological Chemistry*, 278, 23094-23100.

Pahl, H.L. (1999) Activators and target genes of Rel/NF-κB transcription factors. *Oncogene*, 18, 6853-6866.

Vallabhapurapu, S. and Karin, M. (2009) Regulation and function of NF-κB transcription factors in the immune system. *Annual Review of Immunology*, 27, 693–733.

Wei, H., Wang, B., Miyagi, M., She, Y., Gopalan, B., Huang, D.B., Ghosh, G., Stark, G.R. and Lu, T. (2013). PRMT5 dimethylates R30 of the p65 subunit to activate

NF-κB. *Proceedings of the National Academy of Sciences of the United States of America*, *110*(33), 13516–13521.

Xia, Y., Shen, S. and Verma, I.M. (2014) NF-κB, an active player in human cancers. *Cancer Immunology Research.* 2(9), 823–830.

Xiao, G., Harhaj, E.W. and Sun, S.C. (2001) NF-κB-inducing kinase regulates the processing of NF-κB2 p100. *Molecular Cell*, 7(2), 401-409.